NAIC-ID(RS)T-0376-96

NATIONAL AIR INTELLIGENCE CENTER

INFLUENCE OF TAPE RECORDER MOTION ON CCD IMAGE

by

Zhao Yang

HUMAN TRANSLATION

NAIC-ID(RS)T-0376-96 1 October 1996

MICROFICHE NR:

INFLUENCE OF TAPE RECORDER MOTION ON CCD IMAGE

By: Zhao Yang

English pages: 14

Source: Chinese Space Science and Technology, Vol. 15, Nr. 4, 1995 (China Astronautics and Missilery Abstracts, Vol. 2, Nr. 5, 1995); pp. 22-29

Country of origin: China
Translated by: Leo Kanner Associates
F33657-88-D-2188
Requester: NAIC/TASC/Lt Lori A. Thorson
Approved for public release: distribution unlimited.

GRAPHICS DISCLAIMER

All figures, graphics, tables, equations, etc. merged into this translation were extracted from the best quality copy available.

INFLUENCE OF TAPE RECORDER MOTION ON CCD IMAGE

Zhao Yang

Beijing Institute of Satellite Information Engineering, Beijing 100081

ABSTRACT:

Abstract In this paper, the simulation model for the mutual influence between the motion of the rotational parts and the satellite attitude vibration is presented by using Lagrange equation, and the satellite attitude is calculated. The influence on the CCD image geometric quality is discussed.

Subject Term Rigid wheel Satellite attitude Vibration Mathematical model Image quality Analyzing

I. Foreword

Along with the progress of economic and defense programs as well as scientific undertakings, requirements of geometric quality of satellite remote sensing pictures (such as resolution power, in regard to geometric anomalies and positioning precision) are higher and higher. Attitude vibration of the satellite is one of important factors affecting geometric quality, especially serious in the case of remote sensing systems applying linear array CCD scan imaging. Therefore, analysis of the effect of satellite attitude on picture quality is one of the important problems concerning designers.

To cope with the continuous progress of space projects, and the more and more complicated dynamic structure of spacecraft, the craft often carry rigid rotating components and elastic bodies such as solar sails. This article analyzes the effect from the rotating tape in a recorder on the geometric quality (such as positioning precision and internal geometric anomalies) of imaging with respect to the satellite-borne CCD multi-spectrum camera.

Generally, a magnetic tape recorder and a CCD camera are installed at the bottom (facing the Earth) of the satellite. The rotating shaft of the recorder tape is parallel to the flight direction. During satellite flight, rotation at constant linear speed is underway. The CCD camera applies the CCD linear array for scan imaging.

During installation deviations of mass center and shaft alignment of the tape recorder wheel may occur. In the rotational process it is required to control torque, which controls the rotational speed. These actions may cause attitude vibration of the satellite and directional deviation of the CCD camera, thus affecting geometric quality of CCD imaging.

In this article, the satellite and its rotational components are considered as a multiple rigid body. By applying a Lagrange equation in quasi-coordinates and another Lagrange equation with Ω for coordinates in generalized sense, a simulation model of the interdependent effect between tape wheel rotation and satellite attitude vibration is established. In addition, attitude vibration of the satellite is computed by using a numerical computation method.

By using an imaging model of the satellite-borne linear array CCD camera [5], the effect of attitude vibration on picture quality is analyzed, to estimate the geometric quality of remote sensing pictures by CCD cameras. Besides analyzing the effect on picture quality due to attitude vibration, the geometric quality of remote sensing pictures with the CCD camera is estimated. The model can also be used to analyze effects on picture quality due to orbital motion, Earth rotation, Earth curvature, Earth projection and other aspects. In the article the situation is taken into consideration that there are two tape wound wheels for each tape recorder.

II. Coordinate System and Signal Table

The Coordinate System

1. The coordinate system $O_rX_rY_rZ_r$ of the principal inertia axis of the recorder wheel: origin O_r is mass center of the recorder wheel; O_rX_r, O_rY_r and O_rZ_r are three principal inertia axes of the wheel. The directions of the three axes are close to the three respective axes of $OX_1Y_1Z_1$.

2. The coordinate system $O_sX_sY_sZ_s$ of the principal inertia axis of the satellite: origin O_s is the mass center of the satellite; O_sX_s, O_sY_s and O_sZ_s, respectively, are three principal inertia axes of the satellite. The directions of the three axes are close to the three respective axes of $OX_2Y_2Z_2$.

3. The coordinate system $OX_1Y_1Z_1$ of the recorder wheel rotating axis: origin O is the combined mass center of the satellite; OZ_1 is parallel to the shaft axis and is rigidly connected to the recorder wheel (pointing in the flight direction); OY_1 points to the direction of Earth's center while OX_1, OY_1 and OZ_1 form a right-handed system.

4. The coordinate system $OX_2Y_2Z_2$ of the satellite rotating axis: origin O is the satellite combined mass center; OZ_2 is parallel to the shaft axis (pointing in the flight direction) and rigidly connected to the satellite; OY_1 points to the direction of the Earth's center while OX_2, OY_2 and OZ_2 form a right-handed system.

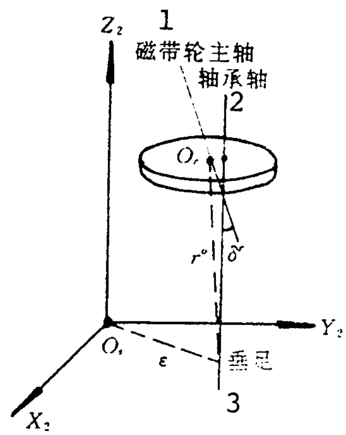

Fig. 1 Diagram Showing a Model of Magnetic Tape Recorder Wheel

Key: 1. Main shaft of recorder wheel; 2. Bearing axis; 3. Foot of perpendicular

Table of Symbols

Superscript and subscript r=a, b, c or d, indicate four recorder wheels respectively;

J_x^r, J_y^r --- horizontal direction inertia of recorder wheel;

J_z^r --- rotating shaft inertia of recorder wheel (under ideal situation as consistent with the shaft axis);

δ^a --- dip angle of recorder wheel A principal axis relative to the shaft axis;

$(\delta^{\omega}_{x1}, \delta^{\omega}_{y1}, 0)^T$ --- projection of δ^{ω} in $OX_1Y_1Z_1$;

J_s --- rotation inertia of satellite;

$$\begin{vmatrix} J^s_{x_2x_2} & J^s_{x_2y_2} & J^s_{x_2z_2} \\ J^s_{y_2x_2} & J^s_{y_2y_2} & J^s_{y_2z_2} \\ J^s_{z_2x_2} & J^s_{z_2y_2} & J^s_{z_2z_2} \end{vmatrix}$$ --- projection of J_s in $OX_2Y_2Z_2$;

m_r --- mass of recorder wheel;

m_s --- satellite mass;

ε --- vertical vector from satellite mass center to shaft axis;

$(\varepsilon_{x2}, \varepsilon_{y2}, 0)^T$ --- projection of ε in $OX_2Y_2Z_2$;

r --- vector from recorder wheel A mass center to satellite mass center;

r^0 --- vector of perpendicular foot on shaft axis from recorder wheel A mass center to satellite mass center;

$(r^o_{x1}, r^o_{y1}, r^o_{z1})$ --- projection of r^0 in $OX_1Y_1Z_1$

L_{x2}, L_{y2}, L_{z2} --- control torque of satellite;

ω --- satellite angular velocity in inertia space;

$(\omega_{x2}, \omega_{y2}, \omega_{z2})^T$ --- projection of ω in $OX_2Y_2Z_2$;

Ω_r --- relative angular velocity of various recorder wheels relative to satellite;

$(0, 0, \Omega_r)^T$ --- projection of Ω in $OX_1Y_1Z_1$;

T --- total kinetic energy of satellite;

$\Phi_r = \Omega_r$

ψ --- rolling angle; θ --- elevation angle; and ϕ --- drift angle.

III. Establishing the Model

3.1 Model of the recorder wheel

In this article, in the satellite are installed two tape recorders with two wheels in each recorder, a total of four recorder wheels, marked as A, B and C, D wheels. A recorder wheel is composed of a disk wound with tape. In the photographic process, the tape of each recorder is wound around another disk (A→B, C→D) while the linear velocity V_0 is constant.

(1) Main rotation inertia of the recorder wheel

$$J' = J_p + J_q$$

J_p is rotation inertia of the recorder wheel while J_q is rotation inertia of the tape. J_q can be calculated from the following equation:

$$J_{zq} = \frac{1}{2}(R_p^2 + R_r^2)M_r$$

$$J_{xq} = J_{yq} = \frac{1}{4}M_r(R_p^2 - R_r^2 + h^2/3)$$

In the equation,

M_r is mass of tape wound around the disk;

R_p is internal radius of the recorder disk;

R_r is radius after tape is wound around the disk; and

h is width of the tape.

(2) Angular velocity and radius of recorder wheel

When starting operation all tapes are wound around wheel A and wheel C. With simultaneous start and reverse rotating direction, finally all tapes are wound around wheel B and wheel D as the following:

$$\Omega_c = -\Omega_a, \quad \Omega_d = -\Omega_b, \quad \Phi_c = -\Phi_a, \quad \Phi_d = -\Phi_b$$
$$\dot{\Omega}_c = -\dot{\Omega}_a, \quad \dot{\Omega}_d = -\dot{\Omega}_b \quad R_c = R_a, \quad R_d = R_b$$

In brief, it is assumed that for each loop of wheel rotation, the wheel radius adds or reduces a layer of tape thickness H=0.0295mm; the angular velocity and angular acceleration are calculated from the following equation

$$\Omega_r = V_0/R_r$$
$$\dot{\Omega}_r = [V_0/(R_r \pm H) - \Omega_r]/(2\pi/\Omega_r) \qquad \text{(subscript r=a, b, c or d)} \qquad (1)$$

(3) Mass of tape wound around the recorder wheel

$$M_a = M_c = M - \rho \cdot V_0 \cdot t$$
$$M_b = M_d = \rho \cdot V_0 \cdot t \qquad (2)$$

In the equations, ρ is mass of a unit length of tape; M is total tape mass wound around a pair of recorder wheels.

3.2 Satellite attitude simulation model

Since the rotating axis of satellite rotation components is not aligned with the principal inertia axis of the satellite, and swing is caused by the deviating rotation axis from mass center position of the rotating components, attitude vibration of the satellite will be induced.

In this section, a Lagrange equation is applied to derive an attitude model of the three-axis stabilized satellite with four recorder wheels. Therefore, the equation can be used to calculate the effect on satellite attitude by recorder wheel rotation.

When establishing the mathematical model, the following aspects are assumed:

1. Both satellite and recorder wheel are rigid, and shafts are rigidly connected;

2. The axis of rotatation of the recorder wheel is inclined while installation position deviates.

(1) Kinetic equation of attitude motion

By using Lagrange equation of $\boldsymbol{\omega}$ in quasi-coordinates, and another Lagrange equation with ϕ as coordinates in the generalized sense, generalized motion equations of the satellite are derived, as follows:

$$\left.\begin{aligned}
\frac{\mathrm{d}}{\mathrm{d}t}\left(\frac{\partial T}{\partial \omega_{x2}}\right) - \omega_{z2}\frac{\partial T}{\partial \omega_{y2}} + \omega_{y2}\frac{\partial T}{\partial \omega_{z2}} &= L_{x2} \\
\frac{\mathrm{d}}{\mathrm{d}t}\left(\frac{\partial T}{\partial \omega_{y2}}\right) - \omega_{x2}\frac{\partial T}{\partial \omega_{z2}} + \omega_{z2}\frac{\partial T}{\partial \omega_{x2}} &= L_{y2} \\
\frac{\mathrm{d}}{\mathrm{d}t}\left(\frac{\partial T}{\partial \omega_{z2}}\right) - \omega_{y2}\frac{\partial T}{\partial \omega_{x2}} + \omega_{x2}\frac{\partial T}{\partial \omega_{y2}} &= L_{z2}
\end{aligned}\right\} \tag{3}$$

To derive the kinetic energy, we substitute into equation (3). Following linearization, attitude kinetic equations used for simulation analysis are derived.

$$\begin{aligned}
&[J^s_{x2x2} + J^a_{x2x2} + J^b_{x2x2} + J^c_{x2x2} + J^d_{x2x2} + \mu(r^0_{z2})^2 + \mu(r^0_{y2} - \varepsilon_{y2})^2]\dot{\omega}_{x2} + \\
&[J^s_{x2y2} + J^a_{x2y2} + J^b_{x2y2} + J^c_{x2y2} + J^d_{x2y2} + \mu(\varepsilon_{x2} - r^0_{x2})(r^0_{y2} - \varepsilon_{y2})]\dot{\omega}_{y2} + \\
&[J^s_{x2z2} + J^a_{x2z2} + J^b_{x2z2} + J^c_{x2z2} + J^d_{x2z2} + \mu r^0_{z2}(\varepsilon_{x2} - r^0_{x2})]\dot{\omega}_{z2} = \\
&L_{x2} - [J^a_{x2z2} - \mu r^0_{z2} r^0_{x2}]\Omega_a - J^b_{x2z2}\Omega_b - J^c_{x2z2}\Omega_c - J^d_{x2z2}\Omega_d - \\
&[\dot{J}^a_{x2x2} + \dot{J}^b_{x2x2} + \dot{J}^c_{x2x2} + \dot{J}^d_{x2x2}]\omega_{x2} - [\dot{J}^a_{x2y2} + \dot{J}^b_{x2y2} + \\
&\dot{J}^c_{x2y2} + \dot{J}^d_{x2y2}]\omega_{y2} - \dot{J}^a_{x2z2}(\omega_{z2} + \Omega_a) - \\
&\dot{J}^b_{x2z2}(\omega_{z2} + \Omega_b) - \dot{J}^c_{x2z2}(\omega_{z2} + \Omega_c) - \dot{J}^d_{x2z2}(\omega_{z2} + \Omega_d) + \\
&\mu r^0_{z2}(\omega_{z2} + \Omega_a)\dot{r}^0_{x2} - \mu(\omega_{x2}\dot{r}^0_{y2} - \omega_{y2}\dot{r}^0_{x2})(r^0_{y2} - \varepsilon_{y2}) - \\
&\mu[\omega_{x2}(r^0_{y2} - \varepsilon_{y2}) + \omega_{y2}(\varepsilon_{x2} - r^0_{x2})]\dot{r}^0_{y2} + \\
&\omega_{z2}[J^a_{y2z2} - \mu r^0_{y2} r^0_{z2}]\Omega_a + \\
&\omega_{z2}[J^b_{y2z2}\Omega_b + J^c_{y2z2}\Omega_c + J^c_{y2z2}\Omega_c + J^d_{y2z2}\Omega_d] - \\
&\omega_{y2}[J^a_{z2z2} + \mu r^0_{y2}(r^0_{y2} - \varepsilon_{y2}) + \mu r^0_{x2}(\varepsilon_{x2} - r^0_{x2})]\Omega_a - \\
&\omega_{y2}[J^b_{z2z2}\Omega_b + J^c_{z2z2}\Omega_c + J^d_{z2z2}\Omega_d]
\end{aligned} \tag{4}$$

$$
\begin{aligned}
&[J^s_{x2y2} + J^a_{x2y2} + J^b_{x2y2} + J^c_{x2y2} + J^d_{x2y2} + \mu(\varepsilon_{x2} - r^0_{x2})(r^0_{y2} - \varepsilon_{y2})]\dot{\omega}_{x2} + \\
&[J^s_{y2y2} + J^a_{y2y2} + J^b_{y2y2} + J^c_{y2y2} + J^d_{y2y2} + \mu(r^0_{z2})^2 + \mu(\varepsilon_{y2} - r^0_{x2})^2]\dot{\omega}_{y2} + \\
&[J^s_{y2z2} + J^a_{y2z2} + J^b_{y2z2} + J^c_{y2y2} + J^d_{y2z2} + \mu r^0_{z2}(\varepsilon_{y2} - r^0_{y2})]\dot{\omega}_{z2} = \\
&L_{y2} - [J^a_{y2z2} - \mu r^0_{z2} r^0_{y2}]\dot{\Omega}_a - J^b_{y2z2}\dot{\Omega}_b - J^c_{y2z2}\dot{\Omega}_c - J^d_{y2z2}\dot{\Omega}_d - \\
&[\dot{J}^a_{x2y2} + \dot{J}^b_{x2y2} + \dot{J}^c_{x2y2} + \dot{J}^d_{x2y2}]\omega_{x2} - [\dot{J}^a_{y2y2} + \dot{J}^b_{y2y2} + \\
&\dot{J}^c_{y2y2} + \dot{J}^d_{y2y2}]\omega_{y2} - \dot{J}^a_{y2z2}(\omega_{z2} + \Omega_a) - \\
&\dot{J}^b_{y2z2}(\omega_{z2} + \Omega_b) - \dot{J}^c_{y2z2}(\omega_{z2} + \Omega_c) - \dot{J}^d_{y2z2}(\omega_{z2} + \Omega_d) + \\
&\mu r^0_{z2}(\omega_{z2} + \Omega_a)\dot{r}^0_{y2} - \mu(\omega_{x2}\dot{r}^0_{y2} - \omega_{y2}\dot{r}^0_{x2})(\varepsilon_{x2} - r^0_{x2}) + \\
&\mu[\omega_{x2}(r^0_{y2} - \varepsilon_{y2}) + \omega_{y2}(\varepsilon_{x2} - r^0_{x2})]\dot{r}^0_{z2} - \\
&\omega_{z2}[J^a_{x2z2} - \mu r^0_{x2} r^0_{z2})\Omega_a + J^b_{x2z2}\Omega_b + J^c_{x2z2}\Omega_c + J^d_{x2z2}\Omega_d] + \\
&\omega_{x2}[J^a_{z2z2} + \mu r^0_{y2}(r^0_{y2} - \varepsilon_{y2}) - \mu r^0_{x2}(\varepsilon_{x2} - r^0_{x2})]\Omega_a + \\
&\omega_{x2}[J^b_{z2z2}\Omega_b + J^c_{z2z2}\Omega_c + J^d_{z2z2}\Omega_d]
\end{aligned}
\tag{5}
$$

$$
\begin{aligned}
&[J^s_{x2z2} + J^a_{x2z2} + J^b_{x2z2} + J^c_{x2z2} + J^d_{x2z2} + \mu r^0_{z2}(\varepsilon_{x2} - r^0_{x2})]\dot{\omega}_{x2} + \\
&[J^s_{y2z2} + J^a_{y2z2} + J^b_{y2z2} + J^c_{y2z2} + J^d_{y2z2} + \mu r^0_{z2}(\varepsilon_{y2} - r^0_{y2})]\dot{\omega}_{y2} + \\
&[J^s_{z2z2} + J^a_{z2z2} + J^b_{z2z2} + J^c_{x2z2} + J^d_{z2z2} + \mu(\varepsilon_{y2} - r^0_{y2})^2 + \mu(\varepsilon_{x2} - r^0_{x2})^2]\dot{\omega}_{z2} = \\
&L_{z2} - [J^a_{z2z2} - \mu r^0_{y2}(\varepsilon_{y2} - r^0_{y2}) - r^0_{x2}(\varepsilon_{x2} - r^0_{x2})]\dot{\Omega}_a - \\
&J^b_{z2z2}\dot{\Omega}_b - J^c_{z2z2}\dot{\Omega}_c - J^d_{z2z2}\dot{\Omega}_d - [\dot{J}^a_{x2z2} + \dot{J}^b_{x2z2} + \dot{J}^c_{x2z2} + \dot{J}^d_{x2z2}]\omega_{x2} - \\
&[\dot{J}^a_{y2z2} + \dot{J}^b_{y2z2} + \dot{J}^c_{y2z2} + \dot{J}^d_{y2z2}]\omega_{y2} - \dot{J}^a_{z2z2}(\omega_{z2} + \Omega_a) - \\
&\dot{J}^b_{z2z2}(\omega_{z2} + \Omega_b) - \dot{J}^c_{y2z2}(\omega_{z2} + \Omega_c) - \dot{J}^d_{z2z2}(\omega_{z2} + \Omega_d) + \\
&\mu(\varepsilon_{y2} - r^0_{y2})(\omega_{z2} + \Omega_a)\dot{r}^0_{y2} - \mu(r^0_{x2} - \varepsilon_{x2})(\omega_{z2} + \Omega_a)\dot{r}^0_{x2} + \\
&\mu[\omega_{y2} r^0_{z2} + \omega_{z2}\varepsilon_{y2} - (\omega_{z2} + \Omega_a) r^0_{y2}\ ]\dot{r}^0_{y2} - \\
&\mu[(\omega_{z2} + \Omega_a) r^0_{x2} - \omega_{x2} r^0_{z2} - \omega_{z2}\varepsilon_{x2}]\dot{r}^0_{z2} + \\
&\omega_{y2}[(J^a_{x2z2} - \mu r^0_{x2} r^0_{z2})\Omega_a + J^x_{x2z2}\Omega_b + J^c_{x2z2}\Omega_c + J^d_{x2z2}\Omega_d] - \\
&\omega_{x2}[(J^a_{y2z2} + \mu r^0_{y2} r^0_{z2})\Omega_a + J^b_{y2z2}\Omega_b + J^c_{y2z2}\Omega_c + J^d_{y2z2}\Omega_d]
\end{aligned}
\tag{6}
$$

(2) Satellite kinetic equation

To analyze the effect on imaging by attitude motion, it is also required to calculate the attitude angle of the satellite based on angular velocity ω of the satellite relative to inertia space.

Assume that Ω^* is the orbital angular velocity of the satellite, by taking small angle approximations of ψ, ϕ and Ω^*, while neglecting high-order small quantities, equations of satellite attitude motion are obtained.

$$\left.\begin{aligned} \dot{\varphi} &= \omega_x - \Omega^* \cdot \psi \\ \dot{\theta} &= \omega_y - \Omega^* \\ \dot{\psi} &= \omega_z + \Omega^* \cdot \varphi \end{aligned}\right\} \tag{7}$$

IV. Simulation Analysis

4.1 Calculation of attitude variation

The following parameters are picked out in simulation:

Principal rotation inertia of the tape disk:

$$J'_x = 0.008\text{kg}\cdot\text{m}^2,\ J'_y = 0.008\text{kg}\cdot\text{m}^2,\ J'_z = 0.0162\text{kg}\cdot\text{m}^2$$

$$r^0 = (r^0_{x1}, r^0_{y1}, r^0_{z1}) = (2\times10^{-6}\text{m},\ 2\times10^{-6}\text{m},\ 0.2\text{m})^T$$

$$\delta^a = (\delta^a_{x1}, \delta^a_{y1}, 0)^T = (0.0167\text{rad},\ 0.0167\text{rad},\ 0)^T$$

$$\varepsilon = (\varepsilon_{x2}, \varepsilon_{y2}, 0)^T = (0.4\text{m},\ -0.5\text{m},\ 0)^T$$

Take Ω_0 as the initial velocity of recorder wheel.

By using equations (4) through (7), we select parameters and apply the numerical calculation method to derive variation of satellite attitude (see Fig. 2). Then from

$$L_x = (J'_{x2x2}\mathrm{d}\omega_x + J'_{x2y2}\mathrm{d}\omega_y + J'_{x2z2}\mathrm{d}\omega_z)/\mathrm{d}t$$

$$L_y = (J'_{x2y2}\mathrm{d}\omega_x + J'_{y2y2}\mathrm{d}\omega_y + J'_{y2z2}\mathrm{d}\omega_z)/\mathrm{d}t$$

$$L_z = (J'_{x2z2}\mathrm{d}\omega_x + J'_{y2z2}\mathrm{d}\omega_y + J'_{z2z2}\mathrm{d}\omega_z)/\mathrm{d}t$$

we derive the interference torque. See Fig. 3 for calculation results.

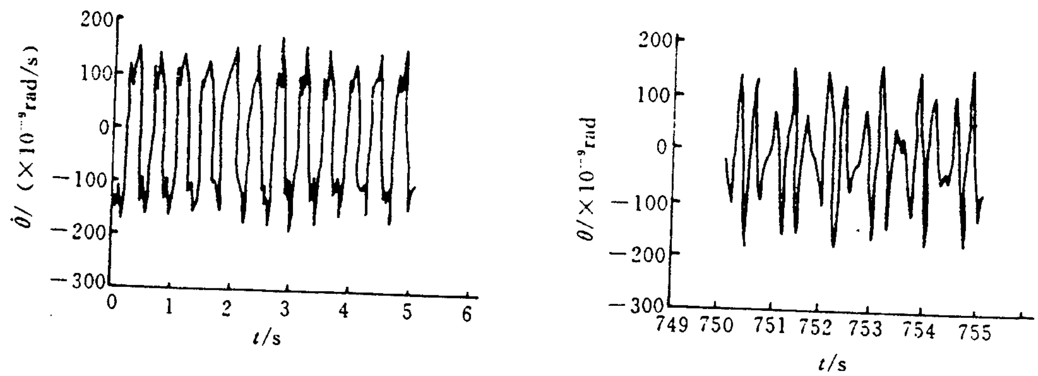

Fig. 2. Satellite attitude variation without considering start process

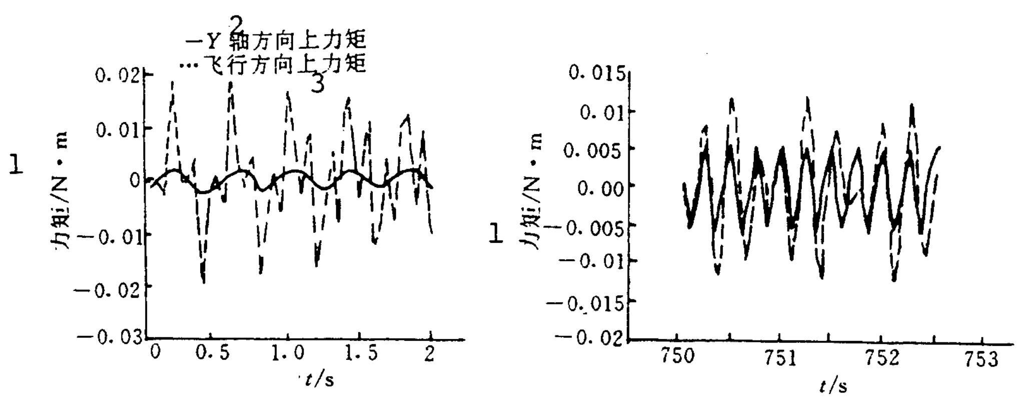

Fig. 3. Interference torque due to rotation of magnetic tape wheel when starting process is not considered

Key: 1. Torque; 2. Torque along direction of Y axis; 3. Torque along flight direction

4.2 Imaging quality of CCD camera

To further analyze the effect on CCD imaging quality by tape recorder operation, the physical process of imaging is applied to establish an imaging model. By using this model and the above-mentioned data of attitude angle, a simulation graph is plotted. Then another simulation graph is plotted by using attitude angle at zero (in the case without recorder wheel rotation) as the standard graph. The picture amplitude is equivalent to 5400 x 5400 picture elements. A point is picked for every 600 picture elements in each line and each row to be used as the control point for precision check.

(1) Calculate mean square deviation of the corresponding points for two pictures

$$\mathrm{DDD} = \left\{\left[\sum (X_i - X_{0i})^2 + \sum (Y_i - Y_{0i})^2\right]/n\right\}^{\frac{1}{2}}$$

In the equation, (X_i, Y_i) is the point in the simulation graph with tape wheel rotation; (X_{0i}, Y_{0i}) is the point in the simulation graph without tape wheel rotation.

These data indicate error in absolute positioning as affected by attitude. See Table 1 for calculation results.

Table 1. CCD imaging indexes of simulation calculation

Condition	DDD	DDTM
Considering start process	0.00608m	0.00376m
No start process	0.01219m	0.00686m

(2) Calculate error from internal anomaly

Mean value of error $$\Delta X = \frac{1}{n}\sum(X_i - X_{0i})$$

$$\Delta Y = \frac{1}{n}\sum(Y_i - Y_{0i});$$

Standard deviation for single-direction error

$$\delta X = \sqrt{\sum[(X_i - X_{0i})^2 - (\Delta X)^2]/(n-1)}$$

$$\delta Y = \sqrt{\sum[(Y_i - Y_{0i})^2 - (\Delta Y)^2]/(n-1)}$$

Standard deviation of error

$$\mathrm{DDTM} = [(\delta X)^2 + (\delta Y)^2]^{1/2}$$

DDTM indicates the relative positioning error due to parameter deviation, thus revealing the internal anomaly of the graph. See Table 1 for calculation results.

Consideration is given to the starting process; that is, when calculating attitude, the initial velocity of the recorder wheel is 0 with consideration of the start process.

When t < 6s,

$$d\Omega_a = -d\Omega_c = V_0/(r_{oa} \times 6)$$
$$d\Omega_d = -d\Omega_b = V_0/(r_{ob} \times 6)$$

Without starting process, that is, during calculations of the attitude, the initial velocity of tape wheel is .

The author expresses his gratitude to guidance by his teacher Guo Shaozeng, as well as enthusiastic support and assistance given by chief engineers Chen Yiyuan and Li Ye, and deputy chief engineer Tan Weichi, along with the following colleagues: Xu Lei, Chang Jijun, Tu Lanjun, Wu Minxing and Chen Yiqing. In addition, the author expresses his gratitude to colleagues at the image evaluation project section and the Beijing Institute of Satellite Information Engineering for their support and assistance.

The article was received for publication on December 8, 1994.

Brief introduction of the author: Zhao Yang, a male, was born in July 1969. He is currently an assistant engineer. He was graduated from Shandong University in 1991. Thereafter, he enrolled in the Beijing Institute as a candidate studying for master's degree. He was awarded a master's degree in July 1994. He has been working at the institute since then.

References

1 郭兆曾．双自旋卫星的姿态运动和控制．宇航学报，1981（4）

2 Mcinture J E，Gianelli M J. Bearing axis wobble for a dual spin vehicle. Journal of spacecraft and rocket，1971，8（9）

3 陆元九．陀螺及惯性导航原理（上）．科学出版社（第二版），1976.

钱伟长．变分法及有限元（上）．科学出版社，1980.

5 赵阳．太阳帆板振动对星载 CCD 相机成像的影响．中国空间科学技术，1995，15（2）：32～39